NUCLEAR SCIENCE AND TECHNIQUES **25**, 060103 (2014)

Development of button-type pickup for SSRF ring*

ZHAO Guo-Bi (赵国璧),[1] YUAN Ren-Xian (袁任贤),[1] CHEN Zhi-Chu (陈之初),[1]
ZHOU Wei-Min (周伟民),[1] and LENG Yong-Bin (冷用斌)[1,†]

[1]*Shanghai Institute of Applied Physics, Chinese Academy of Sciences, Shanghai 201800, China*
(Received January 23, 2013; accepted in revised form March 18, 2014; published online December 15, 2014)

In building Shanghai Synchrotron Radiation Facility (SSRF), in order to reduce or eliminate the unnecessary sources of beam motion, the precise and stable beam position measurement system in the feedback system was required. In this study, we focused on theoretical analysis of the electrode of beam position monitor (BPM). Simulations, including analytic derivations of the propagation impedance and the distribution inductance, were performed. The BPM was designed based on the results and the acceptance measurements of the impedance and the inductance by using the time domain reflection (TDR) with a network analyzer. It has been proved in years of operations that the BPM system meets the requirement of the resolution of sub-micron.

Keywords: SSRF, BPM, Position sensitivity, Cut-off frequency, Distributed capacitance

DOI: 10.13538/j.1001-8042/nst.25.060103

I. INTRODUCTION

Shanghai Synchrotron Radiation Facility (SSRF) has a storage ring of a 432 m in circumference, operating at 3.5 GeV [1]. During its commissioning and routine operation, the button-type BPMs play a key role. They ensure its stable high performance operation, and provide position information to the orbit feedback system, the transverse feedback system, and the safety interlock system, etc., in required precisions and rates. Especially, the high precision closed orbit position feedback system tracks the position in a resolution of 1 μm @ 2 Hz bandwidth, the transverse feedback system needs the bunch-by-bunch position signal in resolution of 10 μm @ 250 MHz bandwidth, and the measurements of turn-by-turn signal need the resolution and data rate in between the above two. For the BPM detector itself, the main technical difficulty of implementation is to ensure the bunch-by-bunch signal with high signal-to-noise ratio (SNR) while avoiding the beam impedance mismatch and the higher order mode (HOM) excitation. In this paper, according to the beam parameters of SSRF, we discuss detailed technical issues involved in the BPM design.

TABLE 1. Beam parameters of the SSRF storage ring [2, 3]

Parameters	Numerical value
Revolution frequency (kHz)	694
Harmonic number	720
Beam current	200–300 mA @ multi bunch mode $<$ 5 mA @ single bunch mode, Phase I $<$ 20 mA @ single bunch mode, Phase II
RF Frequency (MHz)	499.654
Bunch length (mm)	4.32
Natural emittance (nm rad)	4.8
Beam position stability	Better than 1 μm@ 2 Hz bandwidth
Vacuum (torr)	1×10^{-9}

TABLE 2. Specification of the button pickup [2, 4]

Parameter	Requirement
Alignment accuracy	$<$ 200 μm
Signal power @ 499.654 MHz	>-80 dBm @ 0.03 nC $<$ 0 dBm @ 300 mA
Sensitivity	$>$ 0.05 mm^{-1} and $<$ 0.09 mm^{-1}
Beam charge dynamic range	0.02 $\sim$ 300 mA
Position measurement range	±5 mm
Vacuum leakage	$<1\times10^{-10}$ torr Ls^{-1}

II. DESIGN OBJECT

In different cases of SSRF's commissioning and routine operation, the button-type BPM provides position information in different precisions and rates. Table 1 shows the major beam parameters of SSRF accelerator.

The requirements for the button-type BPM differ slightly in different stages of accelerator operation: in the preliminary commissioning stage, higher beam charge sensitivity (larger button size) and higher position sensitivity are required due to small beam charge and large orbit distortion; while in the user operation stage, lower beam charge sensitivity (smaller button size) and lower position sensitivity are required due to high average beam current and high position resolution needs. To meet the requirements and to work with beam parameters in Table 1 before providing appropriate signals to the electronics system, the button-type BPM should achieve the specifications in Table 2.

To meet the goals, the BPMs shall be of appropriate sensitivity, size, and inner structure, i.e. they shall be large enough to provide strong signals, but as small as possible to avoid HOM, with appropriate button separation to achieve desired sensitivity, and with an inner structure to transmit the signal. BPM simulations were performed with the MAFIA code for an optimized structure with a balance between the transfer and coupling impedances.

* Supported by the National Natural Science Foundation of China (No. 11375255)
† Corresponding author, lengyongbin@sinap.ac.cn

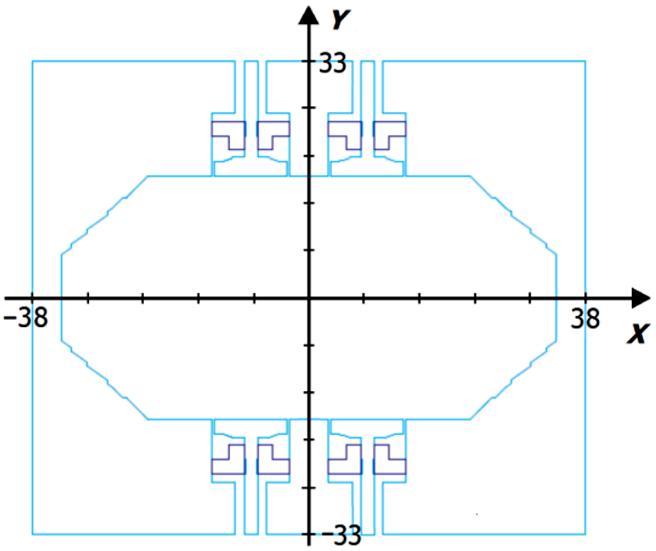

Fig. 1. (Color online) MAFIA geometry of the BPM (in mm).

III. PHYSICAL DESIGNS

The BEPCII BPM simulation [5] is an object lesson in modeling the SSRF BPMs with the MAFIA code (Fig. 1).

A BPM electrode is mounted on inner surface of the beam pipe, The beam pipe geometric structure decides the BPM geometric structure except the BPM electrode size and location. The cross section of the SSRF storage ring beam pipe is octagonal, and the four button electrodes are symmetrically arranged on the upper and lower plane.

The BPM position sensitivities should be as high as possible, and the sensitivities in the horizontal and vertical plane should be as close as possible. The BPM sensitivity is determined by the signals picked up by different electrodes when the beam is off center. We adopt the sensitivity function [6] as

$$S_i = (A - B)/[(A + B)d_i], \tag{1}$$

where S_i and d_i are the offset in the x or y direction, the subscript i denotes either x or y direction; A and B are the signals picked up by the right top and right bottom monitors, respectively.

For BPMs at SSRF, the optimized electrode diameter is 10 mm. The infinite element simulation results are given in the Table 3. G is the distance between the axes of two electrodes on the same horizontal plane; K_x and K_y are position sensitivities in horizontal and vertical planes, respectively; ρ is the normalized line density of induced charge at the electrode center, which is decided by the vacuum chamber structure and the electrode size and position; $g = \rho 2\pi B$ is the shape factor (B is the distance between the electrode center and geometric center of the vacuum chamber), which means the deviation from distribution of induced charge at the electrode center to the circular chamber. As can be seen, by adjusting the relative position of the electrodes, the BPM sensitivities agree in the horizontal and vertical directions.

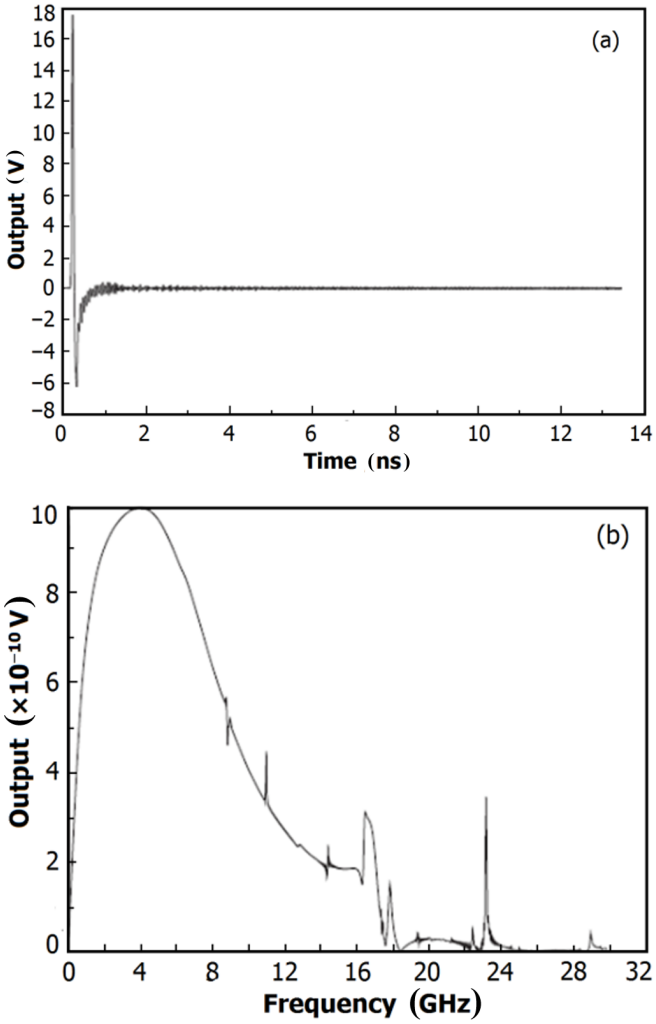

Fig. 2. The output voltage (a) and frequency spectrum (b) of electrode.

TABLE 3. Simulation results of different electrode structures. H-BPM, high precision BPMs; A-BPM, arc area BPM

G	H-BPM (K and ρ in mm^{-1})				A-BPM (K and ρ in mm^{-1})			
(mm)	K_x	K_y	ρ	g	K_x	K_y	P	g
14	0.0784	0.0913	0.0135	1.252	0.0504	0.0786	0.0116	1.340
16	0.0863	0.0847	0.0123	1.179	0.0560	0.0749	0.0109	1.287
18	0.0930	0.0780	0.0111	1.103	0.0610	0.0711	0.0102	1.233

The beam position measurement can be influenced by signal intensity of electrode output. The signal intensity must be big enough to meet the input power requirements of the signal processing electronics, and should not be too strong to break the vacuum sealing when BPMs work under the large current. Finally, we chose $G = 16$ mm.

Button pickup needs to work properly in single bunch mode with low current of 0.02 mA and in multi-bunches mode with high current of 300 mA. The requirement of signal processing electronics is that the input signal power is larger than -85 dBm and smaller than 5 dBm in the bandwidth of

9 MHz. Combined with the insertion loss (around 5 dB) of signal cables, this requirement is larger than −80 dBm and smaller than 0 dBm for pickup output. Fig. 2 shows the output voltage and frequency spectrum of electrode with 10 mm diameter and single bunch charge 1 nC.

The output power (P) in working frequency for the signal processing electronics is

$$\bar{P} = \frac{U^2(\omega_0) \cdot \Delta\omega}{R \cdot \Delta t}, \tag{2}$$

where, U is the output voltage of the corresponding spectrum and varies with ω_0 (the center frequency of signal processing electronics), $\Delta\omega$ is the work bandwidth, R is 50 Ω and Δt is the revolution time. With ϕ10 mm button BPM, spectral intensity of the signal processing electronics is 5.5×10^{-10} V/Hz in center frequency in single bunch operation of SSRF. The output signal power (Fig. 3) of electrode at different beam currents fully satisfies SSRF operation in different conditions.

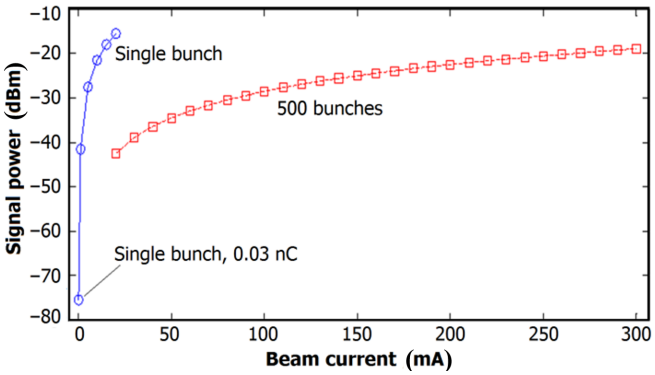

Fig. 3. (Color online) The output signal power of electrode.

HOM brings problems [7, 8]. The TE_{10} mode of beam pipe may cause error in the beam position measurement. The pipe length and height should be considered (height = 10 mm, length < 175 mm). The TE_{10} mode within the cut-off frequency (< 499.654 MHz) will reduce the BPM resolution. The higher slot will cause more transverse impedance. From calculations of the TE_{10} mode, the cut-off frequencies of the higher order modes within the pipe structure are 2.449, 4.412, 4.732, 4.800, 5.464, 6.322, 6.729, 7.220, 8.201 and 8.259 GHz. They are much larger than the center frequency of signal processing(499.654 MHz), so the TE mode, which will be coupled into the signal processing circuit-through BPM electrode, cannot be excited, i.e., the TE mode will not affect the position measurement system.

Simulations were done on influence of the longitudinal wakefield, too. The results are shown in Fig. 4. By integrating the wakefield energy loss, the energy loss factor of the BPM structure is $k = 0.0166$ V/pC. In general, the energy loss factor is particularly sensitive to the electrode size and the gap between the electrode and vacuum tube wall. To prevent large beam loss power, and considering the BPM machining and beam loss power, a 0.3-mm gap is chosen.

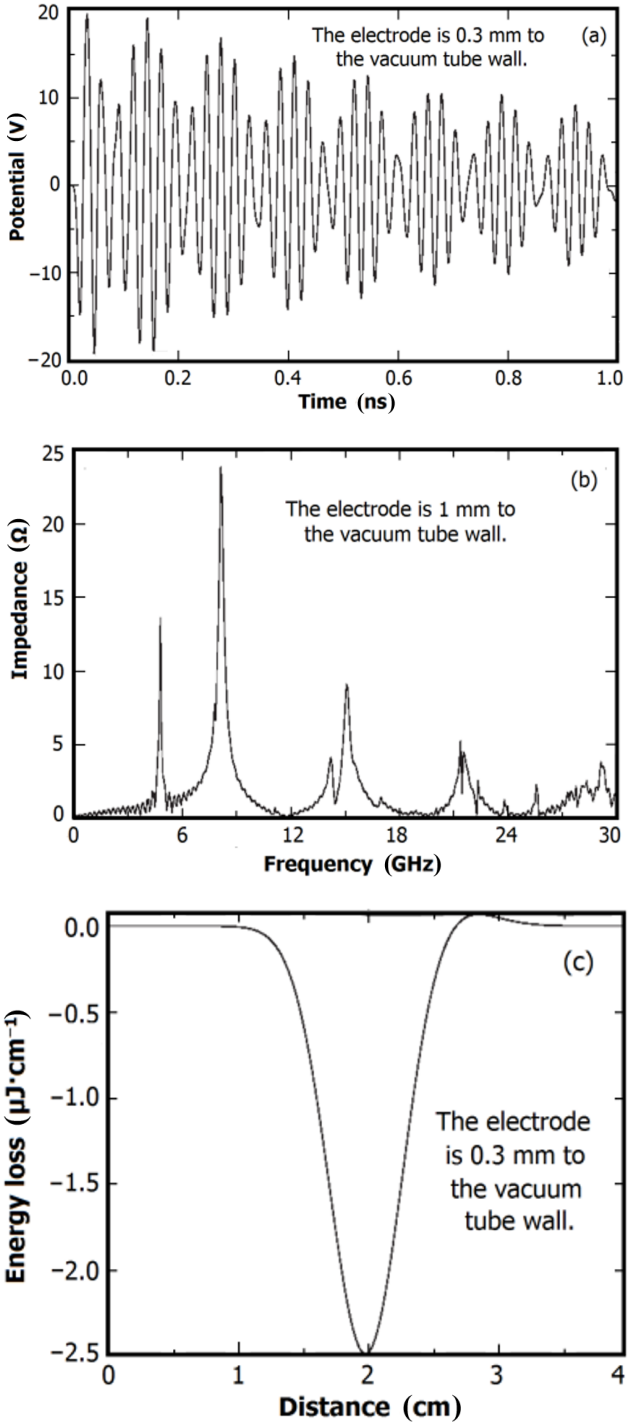

Fig. 4. Wakefield potential within BPM (a) (Amplitude @ 499.654 MHz is 4.6×10^{-10} V/Hz/nC, the product of impedance abscissa and the speed of light is the frequency value), wakefield impedance (b) and energy loss caused by wakefield when the bunch passes the BPM (c).

IV. TECHNICAL DESIGNS

For technological design and tolerance error, we mainly consider impedance matching of the ceramic sealing section

and electrode capacitance. The induced BPM signals are transferred a vacuum seal ceramic section. Its structure must match the characteristic impedance of the signal transmission path, so as not to cause complex higher order mode and coupling problems [7, 8]. Two ways can be used to realize the impedance matching of the segment structure: to make gradual transition of both the inside and outside of the conductor structure, and to shield dielectric transition. Referring experiences of other accelerator labs, the ceramic sealing structure of shielding medium transition (Fig. 5) is used. The ceramic welding in vertical direction is divided into two sections, and the ceramic section welded with outer conductor has a certain degree of freedom in the inner conductor direction, and vice versa, which avoids the welding or normal working thermal expansion damage to the ceramic structure.

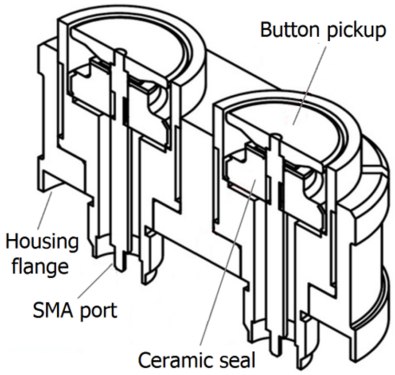

Fig. 5. The shielding medium transition with the ceramic sealing structure of SSRF.

In order to avoid the reflection of incident electromagnetic field in different transmission structure, the characteristic impedance matching should be considered. For the SSRF ceramic structures, when its characteristic length is about the same as transmitted electromagnetic wavelength, even smaller, its characteristic impedance can be analyzed by using TEM mode field structure. For upper part of the ceramic structure, its characteristic impedance, capacitance and other parameters, can be obtained by the equivalent dielectric constant. For the TEM model, assuming the unit length of the inner conductor with free charge q, then by Maxwell equation, the surrounding electric field is

$$E(r) = \frac{q}{2\pi\varepsilon r}, \tag{3}$$

where, r is the radial distance from the center of the inner conductor, and ε is the dielectric constant of this point. After the electric field integral, the voltage difference between inside and outside conductor is

$$V = \frac{q\ln(c/a)}{2\pi\varepsilon_1} + \frac{q\ln(b/c)}{2\pi\varepsilon_2}, \tag{4}$$

where a is the the center conductor radius, b is the inner radius of outer conductor, c is the Ceramic medium radius.

Therefore, we consider the mixed medium as a single medium, and its equivalent dielectric constant $\varepsilon_{\rm eq}$ is

$$\varepsilon_{\rm eq} = \frac{\varepsilon_1\varepsilon_2\ln(b/a)}{\varepsilon_2\ln(c/a) + \varepsilon_1\ln(b/c)}. \tag{5}$$

Therefore, the characteristic impedance and distributed capacitance of the structure is given by

$$Z_c = \frac{60}{\sqrt{\varepsilon_{\rm eq}}}\ln(b/a), \tag{6}$$

$$C = \frac{2\pi\varepsilon_{\rm eq}}{\ln(b/a)}. \tag{7}$$

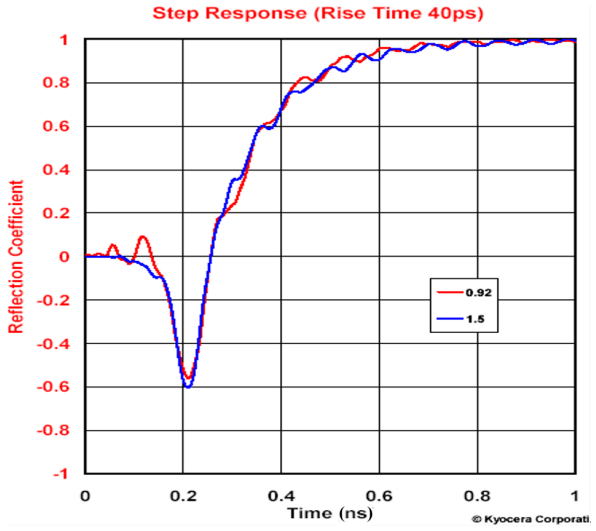

Fig. 6. (Color online) The TDR test results of SSRF BPM upper part ceramic structure before and after the optimized outer diameter (0.92 mm and 1.5 mm) of the inner conductor (Photo courtesy by the Kyocera Corp of Japan).

Figure 6 shows the results of TDR (Time Domain Reflection) test for the upper part ceramic structure before and after optimizing outer diameter of the inner conductor. Equivalent dielectric constant is used in the optimization. The optimized BPM characteristic impedance achieves a smoother transition.

The impedance of BPM wakefield is inversely proportional to its ground capacitance, mainly decided by the electrode ground capacitance. Also, the distributed capacitance of the ceramic dielectric section has a greater contribution to the ground capacitance. For the coaxial structure, the ground capacitance can be calculated by:

$$C = \frac{2\pi\varepsilon\cdot H}{\ln(1+gap/r)}, \tag{8}$$

where, ε is dielectric constant of the medium, H is length of the structure, and gap is the gap between internal and external conductors. For the BPM, the distributed capacitance of electrode is 954 pF/m, equivalent dielectric constant of the upper part ceramic structure is 5.3, the corresponding characteristic

impedance is 50.2 Ω, the coaxial capacitance is 150 pF/m, the lower part ceramic structure equivalent dielectric constant is 2.55, the corresponding characteristic impedance is 66 Ω, the coaxial capacitance is 80 pF/m, and the total capacitance is about 2.4 pF.

Distributed capacitance of the electrode structure can be given by the rise time by TDR test, which is 244 ps when BPM electrode terminal is open (10–90%), for the input impedance of 50 Ω, or electrode capacitance of 2.2 pF, it is consistent with theoretical expectations.

Manufacture error is inevitable. To guarantee the button capacitance, tolerance error of the gap between the round disc and the beam pipe is (300 ± 25) μm, the error in button positioning is 0.1 mm, the reading errors in manufacturer are 0.025 mm and 0.1 mm on X and Y direction, respectively. The error can be adjusted by mapping test or BBA.

Fig. 7. (Color online) The prototype pickup assembly.

TABLE 4. The mainly test items of the button BPM assembly

Test/inspection item	Inspection method	Result
Hermeticity	Helium leak detector	$< 1 \times 10^{-11}$ Pa m^3/s
Reflection coefficient	TDR scope	< 0.01
Button capacitance	LCR meter	< 2.6 pF
Electric impedance	TDR scope	(50 ± 2) Ω

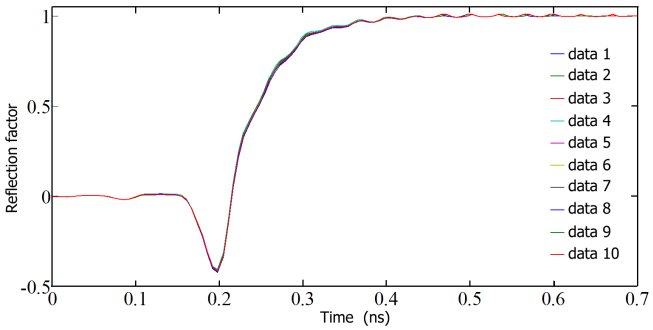

Fig. 8. (Color online) The BPM step response test.

V. FACTORY ACCEPTANCE TEST

The completed assembly unit is shown in Fig. 7. Test inspections were performed to confirm that completed product condition satisfies the required quality. The results are shown

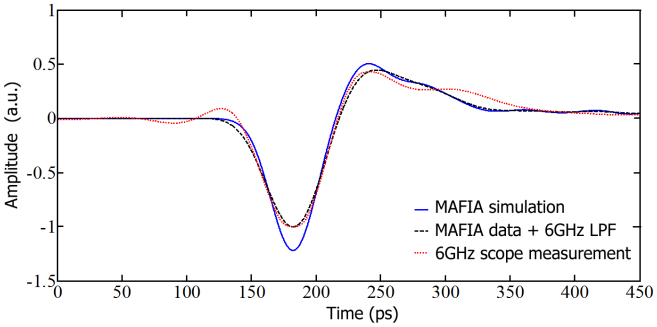

Fig. 9. (Color online) Button signal with a 2.5 mA single-bunch in the storage ring. The measurement is perfect matched with simulation.

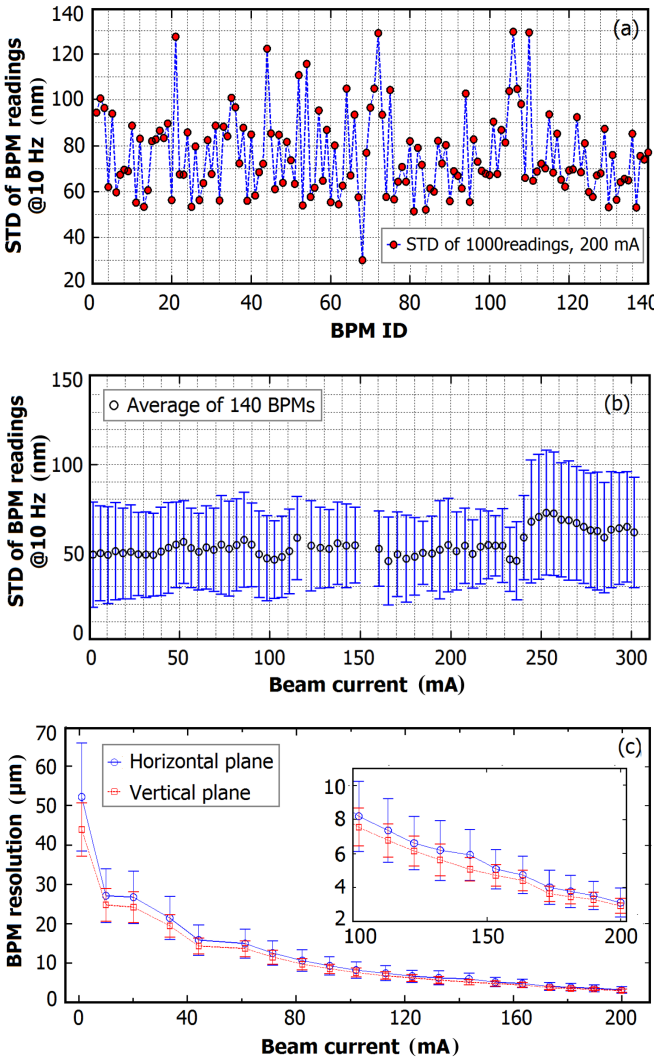

Fig. 10. (Color online) Position resolution of 140 BPMs @ 10 Hz rate (a); and their average position resolution@ 10 Hz rate (b) and @ turn by turn rate (c), as function of the beam current.

in Table 4. As an example, the result of step response inspection of 10 random sampled units, which is performed using TDR scope, is shown in Fig. 8. The BPM performs excellently and consistently. The tests prove that the products fully meet our design goals.

VI. PRACTICAL APPLICATION

A total of 140 sets of BPMs have been implemented in the SSRF storage ring ever since their onsite inspection in 2007. Various types of operation mode, including single bunch with low charge of 0.03 nC, 500 bunches with high current of 300 mA and different hybrid filling modes, have been performed during past six years, and the BPM system is proved to be a great success. Fig. 9 shows the signal from one button measured with a low current single-bunch in the storage ring, which perfectly agrees with theoretical expectation.

The spatial resolutions of narrow band (10 Hz data rate, 2 Hz bandwidth) and broad band (694 kHz data rate, 347 kHz bandwidth) BPM data have been evaluated during user operation. The evaluation results show that sub-microns resolution for slow data (Figs. 10(a) and 10(b)) and microns level resolution for fast data (Fig. 10(c)) have been achieved.

VII. CONCLUSION

By simulating structures of the electrode and BPM layouts, sensitivity of the button type BPM design was optimized. The TE_{10} mode study helped suppression of the HOM which would occur in the vacuum chamber. The acceptance test confirmed the simulated electronic characters. The SSRF operations have proved that the BPM system meets the primary requirements, with long-term availability even during hybrid filling modes which often cause heat load problems.

[1] Zhao Z T, Xu H J, Ding H. Status of Shanghai synchrotron radiation facility, PAC2005, May 16–20, 2005, Knoxville, USA, 214–216.
[2] Shanghai synchrotron radiation facility project preliminary design. National Center for Shanghai synchrotron radiation facility (chips) 2001.
[3] Zhao Z T, Xu H J. SSRF: A 3.5 GeV synchrotron light source for China, EPAC2004, Jul. 5–9, 2004, Lucerne, Switzerland, 2368–2370.
[4] Leng Y B, Zhou W M, Chen Y Z, *et al*. Beam instrumentation system development and commissioning in SSRF. EPAC2008, Jun. 23–27, 2008, Genoa, Italy, 1080–1082
[5] Yuan R X, Cao J S, Ma L, *et al*. BPM simulation of BEPCII.
[6] Ng C K, Weiland T, Martin D, et al. Simulation of PEP-II beam position monitors, PAC1995, May 1-5, 1995, Dallas, Texas, USA, 2485 - 2487.
[7] Novokhatski A. Overall HOM measurement at high beam currents in the PEP-II SLAC B-factory, PAC2007, Jun. 25–29, 2007, Albuquerque, USA, 45–47.
[8] Weathersby S, Novokhatski A. BPM Breakdown Potential in the PEP-II B-factory Storage Ring Collider. ICAP09, Aug. 31–Sept. 4, 2009, San Francisco, USA, 363–366.